Proceedings of the Combustion Institute, Volume 29, 2002/pp. 2963–2973

SANDWICH PROPELLANT COMBUSTION: MODELING AND EXPERIMENTAL COMPARISON

P. A. RAMAKRISHNA, P. J. PAUL AND H. S. MUKUNDA
Combustion Gasification and Propulsion Laboratory
Department of Aerospace Engineering
Indian Institute of Science
Bangalore, India 560012

This paper reports reacting fluid dynamics calculations for an ammonium percholrate binder sandwich and extracts experimentally observed features including surface profiles and maximum regression rates as a function of pressure and binder thickness. These studies have been carried out by solving the two-dimensional unsteady Navier-Stokes equations with energy and species conservation equations and a kinetic model of three reaction steps (ammonium perchlorate decomposition flame, primary diffusion flame, and final diffusion flame) in the gas phase. The unsteady two-dimensional conduction equation is solved in the condensed phase. The regressing surface is unsteady and two dimensional. Computations have been carried out for a binder thickness range of 25–125 μm and a pressure range of 1.4 to 6.9 MPa. Good comparisons at several levels of detail are used to demonstrate the need for condensed-phase two-dimensional unsteady conduction and three-step gas-phase reactions. The choice of kinetic and thermodynamic parameters is crucial to good comparison with experiments. The choice of activation energy parameters for ammonium percholrate combustion has been made with stability of combustion in addition to experimentally determined values reported in literature. The choice of gas-phase parameters for the diffusion flames are made considering that (a) primary diffusion flame affects the low-pressure behavior and (b) final diffusion flame affects high-pressure behavior. The predictions include the low-pressure deflagration limit of the sandwich apart from others noted above. Finally, this study demonstrates the possibility of making meaningful comparisons with experimental observations on sandwich propellant combustion.

Introduction

Several models aimed at predicting the regression rate of composite solid propellant have been constructed, taking into account the importance of flame structure, during last three decades. The Beckstead, Derr, and Price (BDP) model [1], for ammonium perchlorate (AP)–based propellants simplified the unsteady combustion process to an equivalent quasi-steady process. Combustion of a single AP particle in an environment of binder was addressed. In this model, the total heat transfer to the propellant surface was contributed in terms of one-dimensional, mutually non-interacting gas-phase (G-phase) flames. The condensed phase (C phase) was treated as quasi-steady and one dimensional. Following this model, variants of this model were proposed at a time when not only computational resources were inadequate, but also incisive experimental data was unavailable. These features have been discussed adequately in the review papers (the latest is of Ramohalli [2]).

Sandwich Model

The two-dimensional analogue of a composite propellant is a fuel-oxidizer sandwich. Experiments have been conducted on AP-binder sandwiches by many investigators with the idea of striking a compromise between the complexity of three-dimensional combustion zones and the naively one-dimensional approximation. Price [3] has presented a valuable overview. Peak linear regression rates and insightful physical observations reported by Price are very useful in the modeling work. Recent work by Brewster and coworkers [4] has inferred that the regression rate is relatively independent of binder thickness (100–450 μm) and primarily a function of pressure ($r \sim p^{0.4}$) in a pressure range of 0.2 to 3.2 MPa. This indicates the importance of diffusion flames in sandwich propellant (SP) combustion in reducing the pressure index to 0.4 from 0.77 for pure AP [5]. The low value of the pressure index is in part due to the tendency of the binder and the curative to form a melt layer [6].

In the last few years, aspects of the interaction between the two-dimensional G-phase flames and binder material in AP SP [7–10] have been explored. A mention of some of the other modeling efforts in this period can be found in the paper by Hegab et al. [9]. The model developed at the Indian Institute of Science [7,8] has many features similar to the one to be presented here, except for the treatment of the

C phase and the assumption of a planar regressing surface. This study brought out the importance of two-dimensional conduction in the C phase, helping to explain some peculiar experimental observations on SP combustion.

Miccio [10] put forward a five-reaction G-phase model, taking into account the SP topology. That study has many shortcomings such as (1) assumption of equal thermal properties for AP and the binder, (2) choosing a value of C-phase specific heat which is one-third of that of the G phase, (3) identical products of AP monopropellant combustion and of AP-binder combustion, (4) assumption of inviscid fluid while accounting for the two-dimensional diffusion of species and temperature, and (5) allowing for regression only in the flow direction and neglecting the lateral momentum equation, even though there are regions in which the lateral momentum equation is as important.

The model proposed by Hegab et al. [9] solves for both the G and C phase, allowing for unsteady, nonplanar regressing surface with appropriate jump conditions across the gas-solid interface. The G-phase model has a premixed AP monopropellant flame and a diffusion flame. The argument made on the choice of periodic sandwich to limit their work without comparison with experiments is unwarranted. The quenched surface profiles [12] of SP show that at pressures above the low-pressure deflagration limit (LPDL) of AP, regions of AP situated far off (5–8 times the conduction layer thickness) from the interface are flat. This implies that heat loss from the edges of SP is insignificant and can be neglected at pressures above LPDL of AP. This aspect has been clearly demonstrated by Nir [11] (refer to Fig. 3 of Ref. [11]). The assumption of constant density [9] leads to large errors, as the temperatures in the G phase change substantially. Although the authors solve the full C-phase equations, the importance of C-phase heat transfer in SP combustion has not been examined.

One of the deficiencies of all the above-mentioned SP combustion modeling studies is that the AP monopropellant combustion, for which fairly well-established results are available, is inadequately addressed. It is suggested here that a successful model for SP combustion can be obtained only if AP combustion is predicted with reasonable accuracy.

Thus, the objectives of this paper are: (1) to briefly present the new results of AP monopropellant combustion, (2) to describe the topography of the G-phase flame structure, (3) to make comparison with SP combustion experiments [3,4,6,12], (4) to determine whether the features predicted by the model can explain observed behavior of SP combustion, (5) to bring out the importance of C-phase lateral heat transfer in SP combustion, and (6) to elicit the relative importance of the diffusion flames in different pressure regimes.

Mathematical Formulation

The computational domain is the region above and below the pyrolysing surface of the fuel-oxidizer sandwich. The height of the domain above the surface is chosen such that the outer boundary is well above the final diffusion flame. The sandwich is assumed to be an infinite number of alternating binder (hydroxyl terminated poly butadiene [HTPB]) and AP slabs. Symmetry conditions exist along the extended centerline of any binder or AP slab. The time-dependent regressing surface passes through a stack of uniform rectangular grids. During non-uniform regression, the number of cells in the G and C phase is varied adaptively to the evolving surface. This calls for the inclusion of a large number of constant-sized cells next to the regressing surface in the C phase, causing the number of grids in the G phase to increase with surface regression. This problem was partially resolved by having a small number of constant-sized cells in the C phase initially and then adding to it cells as and when required. Similarly, the number of cells in the G phase was reduced when their number increased beyond a set value in the lowest regression zones. Despite adopting this strategy, the number of cells in both the C and G phase increased from their initial value to at times twice the number because of non-uniform regression making the solution computationally very intensive.

The G-phase unsteady conservation equations for mass, momentum, energy, and species are solved in primitive variables. The equations are solved using Patankar's algorithm [13]. First, the momentum equations and then the pressure correction equation are solved to satisfy the continuity equation. Density is obtained from the equation of state after solving for the energy and species conservation equations. The temperature of the regressing surface is obtained by solving the surface heat flux condition along the normal to the surface. The C-phase unsteady conduction equation is then solved. The procedure highlighted above is repeated and the solution is allowed to progress in time, until the specified convergence criteria (to be discussed later) are satisfied. Lewis and Prandtl numbers are assumed unity, and the diffusivities of all species are assumed identical.

The Governing Equations

The governing equations with the notations as explained in the nomenclature are as given below.

Continuity Equation

$$\frac{\partial \rho_g}{\partial t} + \frac{\partial \rho_g u}{\partial x} + \frac{\partial \rho_g v}{\partial y} = 0$$

Generalized x,y Momentum, Energy, Species Conservation Equation

$$\rho_g \frac{\partial \phi}{\partial t} + \rho_g u \frac{\partial \phi}{\partial x} + \rho_g v \frac{\partial \phi}{\partial y} = \Gamma\left(\frac{\partial^2 \phi}{\partial x^2} + \frac{\partial^2 \phi}{\partial y^2}\right) + S_i$$

Condensed Phase Heat Transfer Equation

$$\rho_c \frac{\partial T}{\partial t} + \rho_c \dot{r} \frac{\partial T}{\partial x} = \frac{k_c}{C_{pc}}\left(\frac{\partial^2 T}{\partial x^2} + \frac{\partial^2 T}{\partial y^2}\right)$$

Kinetic Details

The AP surface decomposition process is known to occur through a liquid layer (similar to Ref. [14]), with exothermic pyrolysis. It is taken as,

$$\text{AP} \rightarrow (1 - f)\ \text{APP} + (f)\ \text{APD} \qquad \text{(R1)}$$

When the surface temperature goes below 850 K (corresponding to 2.07 MPa pressure and burn rate of 3.3 mm/s [15]), the thickness of the liquid layer begins to decrease and goes to zero when surface temperature equals the melt temperature of 825 K [15]. As the thickness of the liquid layer decreases, the fraction f of ammonium perchlorate pyrolysis products (APP) going to ammonium perchlorate decomposition products (APD) at the surface also decreases and goes to zero at $T_s = 825$ K. This is consistent with the surface decomposition being related to the activity in the liquid layer. The fraction f is taken as 0.6 for $T_s > 850$ K and is assumed to decay linearly for $T_s < 850$ K in conformity with the liquid layer thickness as $f = 0.6 - 0.024(850 - T_s)$ and is zero for $T_s < 825$ K. The surface heat release obtained using the above model is -205 kJ/kg (at 2.07 MPa and $T_{in} = 26$ °C).

The overall reaction scheme (apart from the above) utilized for the surface and G-phase chemical kinetics model, similar to the one described in the BDP model [1], is as given below:

$$\text{HTPB} \rightarrow \text{F} \qquad \text{(R2)}$$

$$\text{APP} \rightarrow \text{APD} \qquad \text{(R3)}$$

$$\text{F} + \beta\ \text{APP} \rightarrow (1 + \beta)\ \text{P} \qquad \text{(R4)}$$

$$\text{F} + \beta\ \text{APD} \rightarrow (1 + \beta)\ \text{P} \qquad \text{(R5)}$$

Reactions R1 and R2 correspond to the AP and binder surface pyrolysis reactions. The G-phase reactions R3, R4, and R5 correspond to AP decomposition process, primary, and final diffusion flames, respectively.

Initial and Boundary Conditions

The initial conditions in the G phase are uniform velocity field with AP pyrolysis products in the region above the AP and fuel vapor in the region above the binder and uniform high temperature to facilitate ignition. A uniform surface temperature corresponding to the velocity field is provided at the regressing surface. The analytical solution corresponding to T_s is taken as initial guess in the C phase.

The boundary conditions at the two sides are symmetry conditions as mentioned earlier, and at the G-phase exit boundary, the diffusive fluxes are taken as zero while allowing for convective fluxes to cross the boundary. Pyrolysis law and the continuity of heat and mass flux constitute the boundary conditions at the pyrolyzing surface. The flux conditions, with the derivatives obtained along the local normal to the regressing surface, are as follows.

$$-\mathcal{D}\rho \left.\frac{\partial Y_i}{\partial \hat{n}}\right|_0^{0^+} = \rho_g u_0 (Y_{iv} - Y_{i0})$$

$$-k_g \left.\frac{\partial T}{\partial \hat{n}}\right|_0^{0^+} = -k_c \left.\frac{\partial T}{\partial \hat{n}}\right|_0^{0^-} + \rho_g u_0 Q_s$$

The pyrolysis law for the surface is $\rho_g u_0 = \rho_c \dot{r} = A_s \exp(-E_s/RT_s)$. The C-phase thickness is chosen to simulate the infinity condition of ambient temperature.

Choice of Parameters

Calculations are made with *variable* thermal properties in the G phase and with temperature averaged thermal properties in the C phase. The temperature averaged thermophysical properties of the C phase utilized in this study are,

H_f of AP [16] = $-2{,}517{,}545$ J/kg

H_f of binder [17] = 363,170 J/kg

C_p of AP [16] = 1602 J/kg K

C_p of binder [18] = 2900 J/kg K

k_c of AP [18] = 0.21 W/m K

k_c of binder [18] = 0.14 W/m K

ρ_c of AP (see in Ref. [14]) = 1950 kg/m^3

ρ_c of binder [18] = 920 kg/m^3

The surface temperature [15] of AP at 2.07 MPa and burn rate of 3.3 mm/s is taken as 850 K. The melt temperature [15] of AP is taken as 825 K.

The G-phase molecular weights of the species are as follows, APP = 117.5, F = 54, APD (NASA SP-273) = 27.8, and P (NASA SP-273) = 26.7.

The heats of formation calculated (inputs from NASA SP-273 and Ref. [19] are APP = -0.48, APD = -3.9, $F = 3.08$, $P = -6.42$, all in M J/k.

The G-phase C_p $(1273.6 - (P - 2.07) \times 1.7$ J/kg K) is taken to vary linearly with pressure to obtain a flame temperature variation of AP monopropellant combustion (NASA SP-273) of 1394–1412 K at a T_{in} of 299 K. The value of $\mathcal{D}\rho$ at any location is obtained

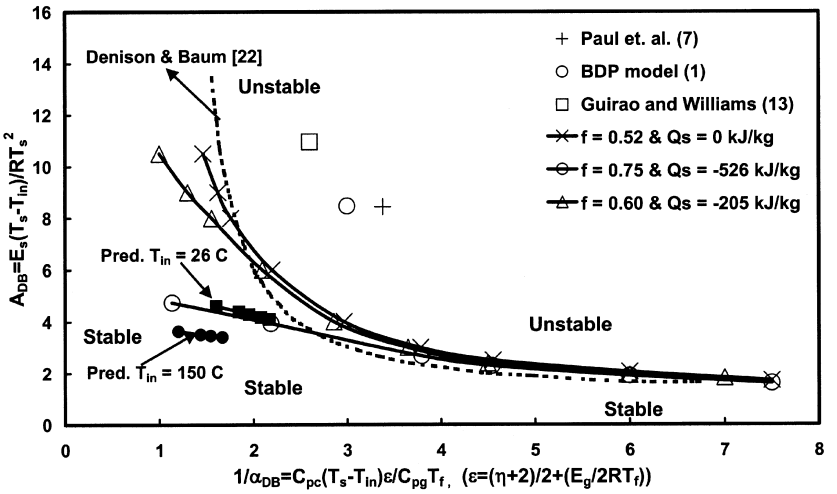

FIG. 1. Predicted results of AP combustion on a plot with the stability parameters of Denison and Baum along with the neutral stability curves due to Denison and Baum [22] and current studies for different values of surface heat release. Predicted results of other models are also plotted.

as a function of temperature at that particular location ($\mathcal{D}\rho \sim T^{0.68}$), and its value at 1000 K is 4.0075 $\times$ 10^{-5} kg/ms. Assumption of unity Lewis and Prandtl numbers is used to obtain values of other G-phase transport properties. The value for E_{sAP} = 50 kJ/mol, although on the lower side of the reported values, is within the range of experimental values reported in the literature [20,21]. The justification for such low values comes from the fact (see Fig. 5.9 of Williams et al. [21]) that in the high burn rate region, the activation energy (extracted as a slope of burn rate versus inverse surface temperature plot) is lower than those encountered at low burn rate regimes. This apart, Fig. 1 shows the neutral stability curves for different surface heat release plotted on stability parameters of Denison and Baum [22]. It is evident from Fig. 1 that an increase in surface heat release shrinks the stable zone, which is consistent with the results of DeLuca and Verri [23]. This forces a lower choice of surface heat release (in turn lower f) and a lower value of activation energies. Current values are chosen after conducting parametric studies (not described here for brevity) to obtain the correct n and σ_p, along with stability of AP monopropellant combustion. A single-step G-phase reaction model has been utilized in the study of AP combustion. The choice of E_{gAP} = 27.5 kJ/mol has been made for reasons noted earlier. The pre-exponential factors for AP surface pyrolysis and decomposition reaction have been tuned to obtain a burn rate of 3.3 mm/s at T_s = 850 K and pressure of 2.07 MPa. The value of E_{bs} = 100 kJ/mol is within the range of values reported in the literature [24]. Around 100 numerical experiments were conducted at various pressures and binder thicknesses before choosing the parameters of the diffusion flame reaction rate and A_s of binder. These along with other parameters discussed above are as given below;

AP surface pyrolysis (R1):

$$A_s = 7864 \text{ kg/m}^2 \text{ s}, \quad E_s = 50 \text{ kJ/mol}, \eta = 0$$

Binder surface pyrolysis (R2):

$$A_s = 1.82 \times 10^7 \text{ kg/m}^2 \text{ s},$$

$$E_s = 100 \text{ kJ/mol}, \eta = 0$$

AP decomposition flame reaction parameters (R2):

$$A_g = 8.55 \times 10^5 \quad E_g = 27.5 \text{ kJ/mol}, \eta = 2$$

Primary diffusion flame reaction parameters (R4):

$$A_g = 4 \times 10^9 \quad E_g = 120 \text{ kJ/mol}, \eta = 1$$

Final diffusion flame reaction parameters (R5):

$$A_g = 5 \times 10^5 \quad E_g = 60 \text{ kJ/mol}, \eta = 1.6.$$

The thermophysical properties chosen are those of HTPB, due to non-availability of the same for polybutadiene acrylonitrile acrylic acid (PBAN). It is expected that these properties are not different for PBAN as the experimentally measured burning rates [6] are in the same range. Besides, it is pertinent to note that the model presented here has no provision to account for binder melt flow and hence cannot make detailed comparison with HTPB, which is reported to cause melt flow [6]. Hence, detailed comparisons will be made with experiments utilizing PBAN as binder.

Grid and Time Step Details

The cells are geometrically stretched in both the C and G phase from the burning surface to the exit

plane in the streamwise (y) direction as given below: at 2.1 MPa: G phase, 0.2–33 μm, C phase, 0.2–75 μm; and at 6.9 MPa: G phase, 0.08–18 μm, C phase, 0.08–25 μm. The cells are geometrically stretched from the AP binder interface toward the edges of both binder and AP in the cross-streamwise (x) direction. Typically, for a 25 μm binder thickness, the cell size near the interface is 0.34 μm and is stretched to 3 μm at the binder edge and 8 μm at the edge of AP slab. The number of cells in the G and C phase (y direction) are 110 and 163, respectively, at the start of the calculation and increases as the SP regresses as described earlier. The number of cells in the lateral direction (x direction) varies from 50 to 70. The height and depth of the computational domain above and below the burning surface is 670 μm and 2.1 mm, respectively, at 2.1 MPa and 257 and 700 μm, respectively, at 6.9 MPa. The AP slab thickness used in all cases is about 10 times the conduction layer thickness. Solutions obtained are grid and time-step independent.

Results and Discussions

Computations were carried out with AP slab alone initially to validate the code and the constants chosen for AP combustion. The current study is free from the assumptions of quasi-steady G phase, thin flame, or constant density. The results obtained have been found to be stable under all conditions (pressure 2.1–14 MPa and T_{in} = 299–423 K) as seen in Fig. 1. Also seen in Fig. 1 are the results obtained by other investigators (see Ref. [20]), which are on the unstable side with reference to Denison and Baum's [22] neutral stability curve. It is seen that most investigators have chosen high E_{sAP}, based on experimental evidence at low heating rate studies (see Refs. [20,21]). Besides, they have chosen a high E_g for AP decomposition flame (thin flame approximation in most cases), resulting in unstable solution when these values (High E_g and E_s for AP) are used in an unsteady C-phase formulation. These have gone unnoticed because of the convention of utilization of one-dimensional steady analytical solution in the C phase.

The pressure index of AP combustion obtained was 0.77 for pressures ranging from 2.07 to 6.91 MPa and decreased from 6.91 to 13.82 MPa, which is in good agreement with the experimental observations [5]. The σ_p obtained was around 0.0023–0.0024 K^{-1}, which is in reasonable agreement with experimental value of 0.0016–0.0021 K^{-1} [5]. The model correctly predicted LPDL of AP due to the incorporation of the concept of loss of melt layer (surface pyrolysis becoming an endothermic process from an exothermic process), accompanied by transient conduction in the C phase (see Ref. [20] for details).

Computations with the SP configuration were carried out for a range of binder thicknesses (25–125 μm) and pressures (1.4–6.9 MPa). The solution was inferred as converged when the obtained regressing surface profile of SP is invariant with time. To help establish the convergence criterion, it was taken that the regression rates at different cross sections parallel to the AP-binder interface (not along local normal to the surface) settle to a value within 5% of each other (see Fig. 2). In addition, the slope of regression rate with time should tend to zero. Results obtained at 1.4 MPa indicate that the regions of AP located far from the interface are regressing at very low rates. This indicates that the activity is restricted to a region close to the AP-binder interface (Fig. 2a, c) and is consistent with experimental observations of Price et al. [12,6]. Thus, it is appropriate to consider only the regions close to the AP-binder interface at 1.4 MPa, while deciding on the convergence criterion. For pressures higher than LPDL of AP, burn rates at each cross section do settle to a value within 5% of each other as seen in Fig. 2b, d.

The reaction rate contours in the G phase (see Fig. 3b, d) show that with an increase in pressure from 1.4 to 2.1 MPa, the inclination of the final diffusion flame from the vertical is reduced because of the greater participation of AP in the combustion. The other intriguing aspect is that, despite the reduction in pressure from 2.1 to 1.4 MPa, the peak primary diffusion flame reaction rate increases by about 5.5 times and the area of activity of this flame also has increased. The corresponding parameters for the final diffusion flame show a considerable decline. At 1.4 MPa, T_s decreases below T_m, and hence the mass fraction of APP is unity at the surface (surface decomposition process). This increase in the availability of APP and corresponding decrease in APD availability close to surface causes the primary diffusion flame to be preferred at pressures below LPDL of AP. The opposite phenomenon occurs at pressures above LPDL of AP. These observations indicate the importance of primary diffusion flame at pressures below LPDL of AP to SP combustion. The current model with two diffusion flames, based on the experimental observations of Brown et al. [25], predicts the burn behavior of a sandwich propellant at all pressures better than the model of Hegab et al. [9] utilizing a single diffusion flame.

The temperature contours in the G phase (refer to Fig. 3a, c) show that at a pressure of 2.1 MPa, the gradients are quite steep (lines are close to each other) close to the AP-binder interface in comparison to the 1.4 MPa case. Besides, the base of both the diffusion flames is close to the AP-binder interface, leading to larger heat feedback to this region from the G phase. This would imply that the AP-binder interface should lead the regression front; however, a rather interesting small protrusion of AP close to the interface region (Fig. 4a) is obtained at

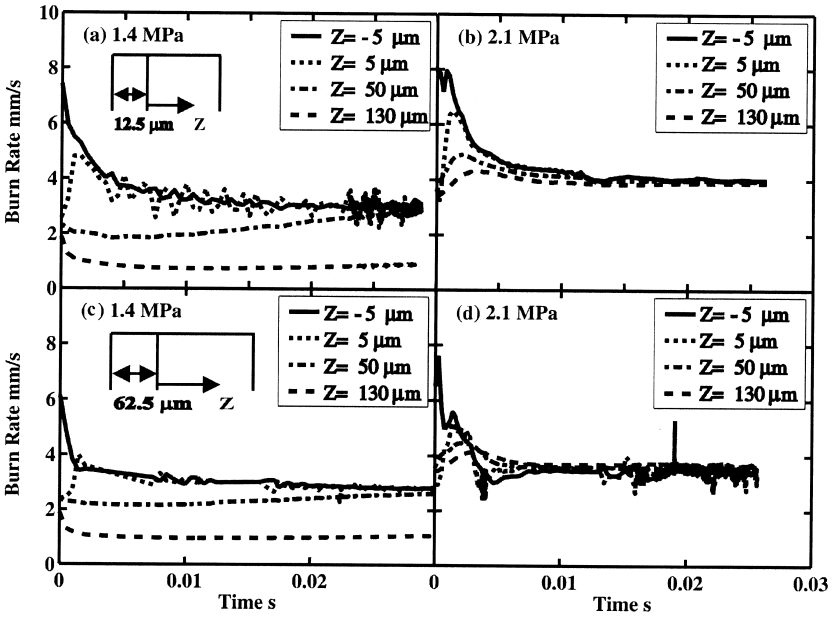

FIG. 2. Burn rates at different cross sections on the surface parallel to AP-binder interface (distances measured from interface as shown) for pressures of 2.1 MPa (b, d) and 1.4 MPa (a, c) and binder thickness of 25 μm (a, b) and 125 μm (c, d).

2.1 MPa. A larger protrusion of AP close to the interface free from froth (smooth band) has been reported in the literature [6,12]. Price et al. [12] have explained this behavior as caused by lateral heat transfer from AP to binder and not binder melt flow as believed earlier (see in Refs. [3,12]). The lower temperature causes a steeper temperature gradient, helping reduce the subsurface temperature in the binder compared to AP, and the C-phase heat transfer from AP to binder takes place, as seen in Fig. 4c. This results in a lower AP temperature and consequently a lower AP burn rate close to the interface. To verify the explanation proposed by Price et al. [12], numerical experiments with raised thermal diffusivity of binder (made equal to that of AP) were carried out. The regression profiles (see Fig. 4b) show no protrusion of AP close to the AP-binder interface as seen in Fig. 4a. The effect of thermal diffusivity of binder on the subsurface temperature is apparent in Fig. 4c, d. This confirms the postulate of Price et al. [12], emphasizing the importance of C-phase conduction on SP combustion.

The predicted surface profiles (Fig. 5) show that at 1.4 MPa, the AP-binder interface leads the regression front. At large binder thicknesses, the binder protrudes out and the protrusion increases with increasing pressure. The predicted surface profiles show that with an increase in pressure, the AP surface tends to become flat irrespective of the binder thickness. These are consistent with the experimental observations of Price et al. [6,12]. The AP surface temperature adjacent to the AP-binder interface is lower than the melt temperature of AP as seen in Fig. 5, and hence the frothy melt layer is absent in this region. Besides, the concentration of APP in the G phase adjacent to the AP-binder interface was high because of the reduced surface decomposition. It is speculated here that the experimentally observed feature of smooth protruding AP surface adjacent to the AP-binder interface is due to the reasons given above.

The predicted variation of the burn rate with pressure and binder thickness (see Fig. 6) is in reasonable agreement with experimental observations [12]. The burn rate is seen to have a maximum value at particular binder thickness, beyond which an increase in binder thickness leads to a decreased burn rate. This suggests that the binder acts mostly as a heat sink, again consistent with experimental findings [12]. The $\boldsymbol{n}$ for SP at maximum regression rate is 0.68 and at large binder thickness limit is 0.74, which is less than the 0.77 observed for AP combustion, indicating the importance of diffusion flames in SP combustion. These numbers are in good agreement with 0.71 and 0.74 at the maximum regression rate and at the large binder thickness limit (PBAN as binder), respectively, of Price et al. Chorpening et al. [4] have reported a lower $\boldsymbol{n}$ of 0.4 (HTPB as binder) at the large binder thickness limit for a variation in pressure from 0.2 to 3.2 MPa. The lower value of $\boldsymbol{n}$ is due to melt layer formation [6] as explained earlier. Current predictions between

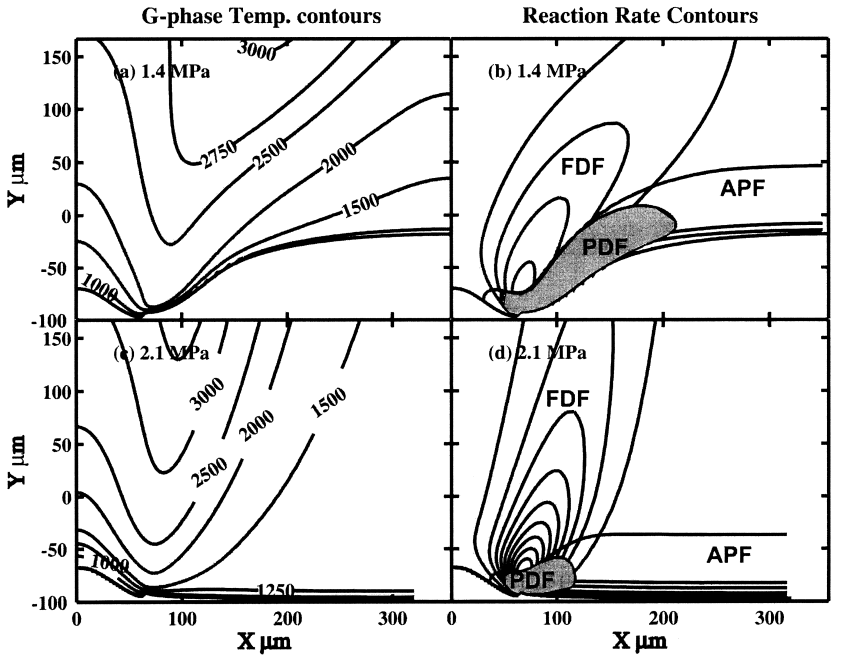

FIG. 3. Gas-phase temperature contours (a, c) and reaction rate contours (b, d) for a pressure of 1.4 MPa (a, b) and 2.1 MPa (c, d) at a binder thickness of 125 μm (half binder thickness 62.5 mm). Position of the flames marked there off (primary diffusion flame shaded). At 1.4 MPa, (b) final diffusion flame reaction rates 2000 (inner ring): 500 (increment): 500 (outer ring) kg/m^3 s, maximum primary diffusion flame reaction rate: 70,000 kg/m^3 s and maximum AP decomposition flame reaction rate: 3.5×10^5 kg/m^3 s. At 2.1 MPa, (b) final diffusion flame reaction rates 8500 (inner ring): 1000 (increment): 500 (outer ring) kg/m^3 s, maximum primary diffusion flame reaction rate: 13,000 kg/m^3 s and maximum AP decomposition flame reaction rate: 3.5×10^5 kg/m^3 s.

1.4 and 2.1 MPa yield a pressure index of 0.73 at large binder thicknesses.

The inclusions of surface liquid layer model for AP and C-phase unsteady heat transfer have resulted in the prediction of regression below LPDL of AP consistent with experimental observations. The final remarkable feature predicted by the model relates to the quenching of SP below a particular binder thickness. As can be clearly seen in Fig. 6, quenching occurs at 10 μm binder thickness compared to the experimental result of 20 μm at 1.4 MPa. This has been possible only through the use of a model with the physical content required to describe the phenomenology and the choice of parameters that explain all the submodels adequately.

Conclusions

Numerical studies of a periodic SP propellant geometry with two-dimensional unsteady G and C phase and a non-planar regressing surface along with a kinetic model of three reaction steps in the G phase have been carried out. The importance of AP monopropellant combustion studies in relation to SP combustion has been brought out. The flame structure over a typical SP has been elucidated, and the importance of a two diffusion flame model over a single diffusion flame model has also been brought out. The importance of two-dimensional C-phase heat transfer in influencing the burn behavior of an SP has been explicitly brought out. The predicted surface profiles are in good qualitative agreement with the experimental observations. The variation of burn rate with binder thickness at different pressures is in good conformity with experimental observations, and the pressure index is 0.68, which agrees well with experimental observations. The prediction of the quenching of the sandwich is indicative of the capture of the appropriateness of the model and the choice of parameters.

Nomenclature

A	pre-exponential factor in both surface pyrolysis law and reaction rate law
APD	equilibrium decomposition products of AP, obtained from NASA SP-273
APP	pyrolysis product of AP (NH_3(gas) + $HClO_4$(gas))

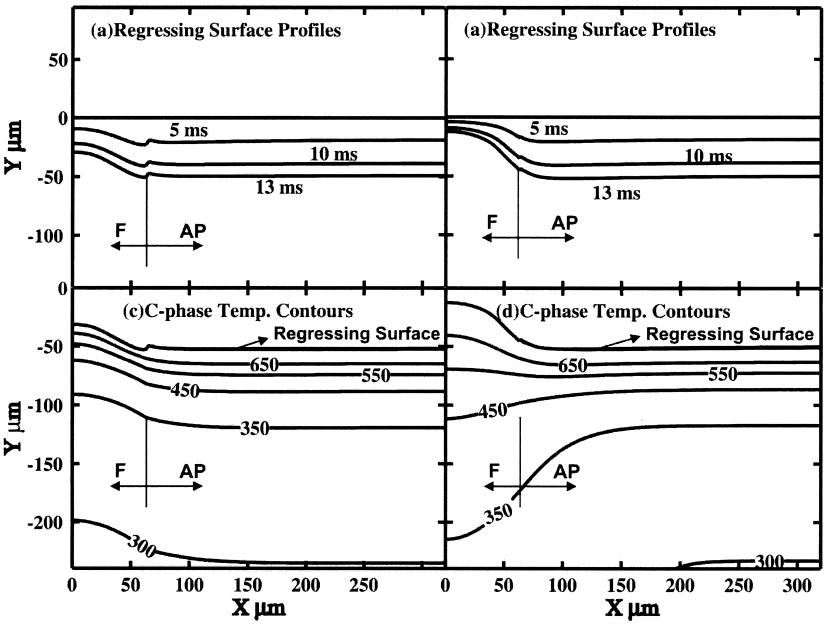

FIG. 4. Regressing surface profiles at various instants (as indicated) for dissimilar AP and binder thermal diffusivity (a) and identical AP and binder thermal diffusivity (b). Corresponding C-phase temperature contours (at 13 ms) are presented in (c and d) respectively for an SP with binder thickness of 125 μm and pressure of 2.1 MPa.

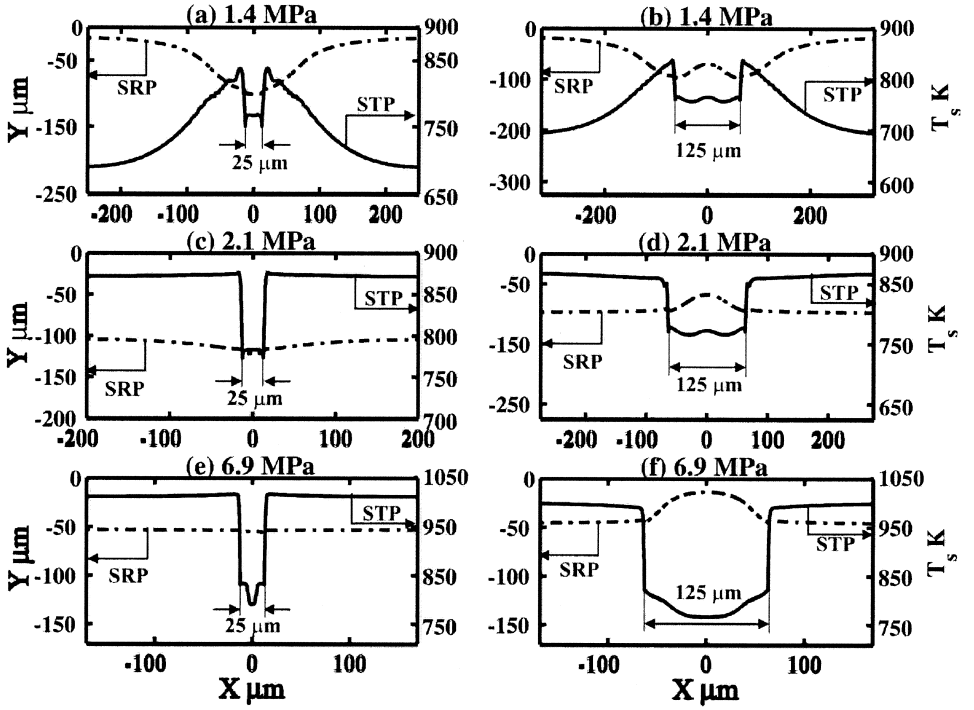

FIG. 5. Surface temperature profile (STP) and surface regressed profile (SRP) of an SP at binder thickness of 25 μm (a, c, e) and 125 μm (b, d, f) for three different pressures of 1.4 MPa (a, b), 2.1 MPa (c, d), and 6.9 MPa (e, f).

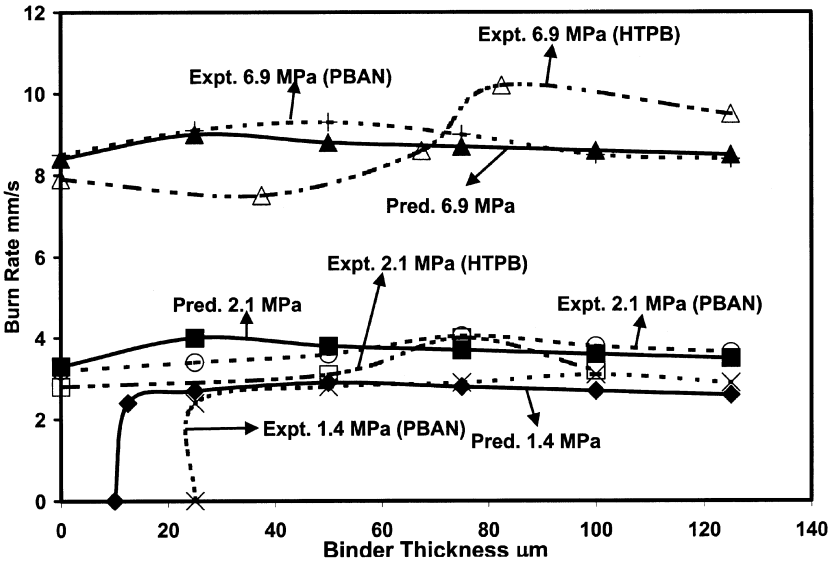

FIG. 6. Variation of burn rate with binder thickness at different pressures for SP along with experimental results of Price et al. [6,12]

C_p	specific heat
$\mathcal{D}$	diffusivity of the species
E	activation energy
F	fuel (C_4H_6)
H_f, H_r	heat of formation, heat of reaction
k	thermal conductivity
n, n̂	pressure index of burn rate in Vieilli's law, local normal
P, p	final products of combustion (NASA SP-273), pressure
Q_s	heat of pyrolysis (positive for endothermic phase change)
R, ṙ	gas constant, burn rate normal to the surface
S_i	source term in the generalized equation $= -(\partial p)/(\partial y)$, $-(\partial p)/(\partial n)$, $-H_r/C\rho\dot{\omega}'''$, $\dot{\omega}_i'''$ for $\phi = u, v, T, Y_i$
T, T_s,T_m,T_{in}	temperature, surface, melt and initial temperature
u, v	velocity of gas in x and y direction, respectively
$\dot{\omega}'''$, $\dot{\omega}_i'''$	overall reaction rate, reaction rate of species i
Y_i	mass fraction of the ith species
β	stoichiometric ratio of oxidizer to fuel = 9.5
ϕ	general variable in the generalized equation = u, v, T, Y_i
Γ	diffusion term in the generalized equation = $\mu, \mu, k/C_p, \mathcal{D}\rho$ for $\phi = u, v, T, Y_i$
η	reaction order
μ	dynamic viscosity of gases
ρ	density
σ_p	initial temperature sensitivity of burn rate

Subscripts

c	condensed phase
g	gas phase
s, sb, sAP	surface pyrolysis, surface pyrolysis–binder, surface pyrolysis–AP
0	at the surface along the perpendicular to the surface
v	pyrolysis product

REFERENCES

1. Beckstead, M. W., Derr, R. L., and Price, C. F., *AIAA J.* 8:2200 (1970).
2. Ramohalli, K. N. R., *Prog. Aeronaut. Astronaut.* 90:409 (1984).
3. Price, E. W., in *Proceedings of the Thirtieth JANNAF Combustion Meeting, Vol.* 2, publication 606, Chemical Propulsion Information Agency, 1993.
4. Chorpening, B. T., Knott, G. M., and Brewster, M. Q., *Proc. Combust. Inst.* 28:847 (2000).
5. Boggs, T. L., and Zurn, D. E., *Combust. Sci. Technol.* 4:227 (1972).
6. Price, E. W., *J. Propul. Power* 4:717 (1995).
7. Mishra, D. P., Paul, P. J., and Mukunda, H. S., *Nat. Conf. Air Breathing Engines Aerospace Propul.* 2:462 (1994).
8. Paul, P. J., Ramakrishna, P. A., and Mukunda, H. S., *Natl. Conf. Air Breathing Engines Aerospace Propul., Vol. 4,* AP 11-21, 1998.

9. Hegab, A., Jackson, T. L., Buckmaster, J., and Stewart, D. S., *Combust. Flame* 125:1055 (2001).
10. Miccio, F., *Proc. Combust. Inst.* 27:2387 (1998).
11. Nir, E. C., *Combust. Flame* 20:419 (1973).
12. Price, E. W., Sambamurti, J. K., Sigman, R. K., and Panyam, R. R., *Combust. Flame* 63:381 (1986).
13. Patankar, S. V., *Numerical Heat Transfer*, Hemisphere, Washington, DC, 1980.
14. Guirao, C., and Williams, F. A., *AIAA J.* 9:1345 (1971).
15. Beckstead, M. W., and Hightower, J. D., *AIAA J.* 5:1785 (1967).
16. Chase Jr., M. W., *NIST-JANAF Thermochemical Tables*, American Institute of Physics, New York, 1998.
17. Robert, H. P., and Cecil, H. C., *Chemical Engineer's Handbook*, McGraw-Hill, Kogakusa, 1973.
18. Zanotti, C., Volpi, A., Bianchessi, M., and DeLuca, L., *Prog. Astronaut. Aeronaut.* 143:145 (1992).
19. Narahari, H. K., "Modeling Studies on Solid Monopropellants," Ph.D thesis, Indian Institute of Science, Bangalore, India, 1986.
20. Ramakrishna, P. A., Paul, P. J., and Mukunda. H. S., *Natl. Conf. Air Breathing Engines Aerospace Propul.* 5:541 (2000).
21. Williams, F. A., Barrere, M., and Huang, N. C., in *Fundamental Aspects of Solid Propellant Rockets*, Technivision Services, Slough, UK, 1969, 253.
22. Denison, M. R., and Baum, E., *Am. Rocket Soc. J.* 31:1112 (1961).
23. DeLuca, L. T., and Verri, M., in *International High Energy Materials Conference and Exhibit, Vol. 3*, 2000, p. 495.
24. Arisawa, H., and Brill, T. B., *Combust. Flame* 106:144 (1996).
25. Brown, W. E., Kennedy, J. R., and Netzer, D. W., *Combust. Sci. Technol.*, 6:211 (1972).

COMMENTS

J. Buckmaster, University of Illinois, USA. There are three points: (1) Ref. [9] in the paper does not employ the constant density assumption. Most of the calculations are carried out using an Oseen approximation in which the flow is described by a time-dependent, spatially varying, parallel shear flow; comparisons with calculations using the full Navier-stokes equations show that this is accurate. (2) It is difficult to see how one could argue that uniform regression (convergence) has been achieved once the regression rates at various points differ by 5%, a large number. And your Fig. 2a shows large and peculiar spikes following a smooth region in the neighborhood of 0.01 s. (3) The form adopted for the viscous stress tensor is only correct for a constant density fluid, as the dilatational term has been omitted.

Author's Reply. We have carefully re-examined Ref. [9]. The paper does not explicitly present the governing equations numerically solved. The discussions on page 1057 of the above reference imply an Oseen approximation in which density is taken constant. The demonstration of accuracy of results by comparison of reaction rate contours between Figs. 9 and 2 is far from being adequate, as the two contour plots are at different time levels and set in different scales. Oseen approximations become invalid at higher pressure and larger binder thickness, as cross-stream-wise flow (v-component) velocities become comparable to stream-wise velocities (see figure below). This is to be expected, as at higher pressures the binder tends to protrude out more leading to a larger v-component consistent with experiments ([Refs. [3,6,12] in paper). Classical Oseen approximation involves the assumption that the perturbation terms are small with respect to the free-stream velocity. The value of free-stream velocity utilized (Ref. [9] in paper) is not indicated, for in stream-wise direction, perturbations will be as large as the free-stream value itself, irrespective of the choice of free-stream value as evident from the following Fig. A:

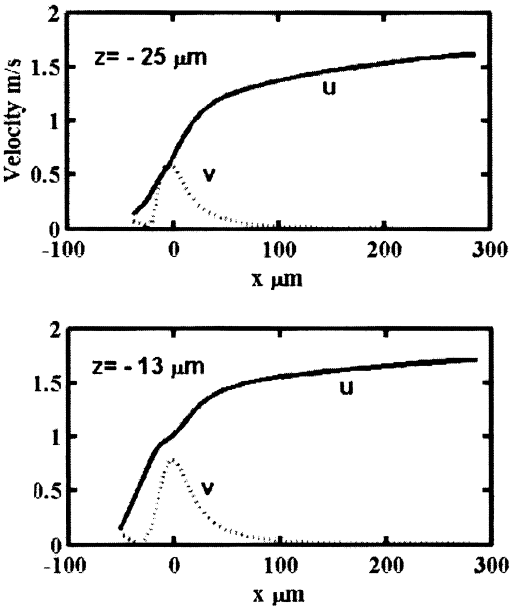

Fig. A. Velocity components (absolute value of v) at locations indicated from the AP-binder interface corresponding to a pressure of 6.9 MPa and binder thickness of 125 μm.

The convergence criteria proposed here is objective and allows the reader to verify whether steady state has been achieved or not, rather than merely stating that stationary state was achieved as in Ref. [9] in the paper. The accuracy of the results in Fig. 2d is assured since it has been verified that these small oscillations do subside with time.

The stress terms associated with the dilation in the momentum equations were dropped, as their contribution was at least three orders of magnitude less than the other stress terms and not due to a constant density assumption. In fact,

a variable density formulation (indicated by the use of equation of state to complete the set of governing equations) has been utilized here.

•

Quinn Brewster, University of Illinois, USA. You showed three early models with the comment that they missed the intrinsic stability prediction due to assuming a quasi-steady, condensed-phase energy equation. I question the (better) description of those models. I can't imagine those models trying to predict such intrinsic stability with a quasi-steady condensed-phase when solid-phase thermal relaxation is the key physical element underlying that phenomenon. Perhaps this is just a question of semantics or terminology.

Author's Reply. The three earlier models shown in the intrinsic stability plot for AP were developed to predict AP combustion and were not developed to predict intrinsic stability. These models had made use of a large surface and gas phase activation energies leading to an unstable solution as depicted in the plot. The comment made was that although the solution was unstable, it went unnoticed due to the use of quasi-steady condensed phase energy equation in these models. Use of an unsteady model would have surely shown the unstable nature of the solution.

•

Oleg P. Korobeinichev, Institute of Chemical Kinetics and Combustion, Russia. In the paper, there is comparison of modeling results only with the experimental data of Dr. E. Price. There is a great deal of other experimental data, for example, of Russian researchers. More comparisons should have been made with other results to check out the model.

Author's Reply. We have compared our results with the experimental results of E. W. Price et al. (Refs. [3,6,12] in paper), Brewster et al. (Ref. [4] in paper) and Brown et al. (Ref. [25] in paper). We are not aware of any work carried out by Russian researchers that present the variation of pure AP-binder sandwich regression rates with pressure and binder thickness such as those reported in the references given in our paper. We look forward to receiving information on any such work and to make comparisons with them in future.